Figure S1. Full images of the western blots used in the present study. (A) Full images of Fig. 2B. (B) Full images of Fig. 2D. (C) Full images of Fig. 3B. (D) Full images of Fig. 3C.

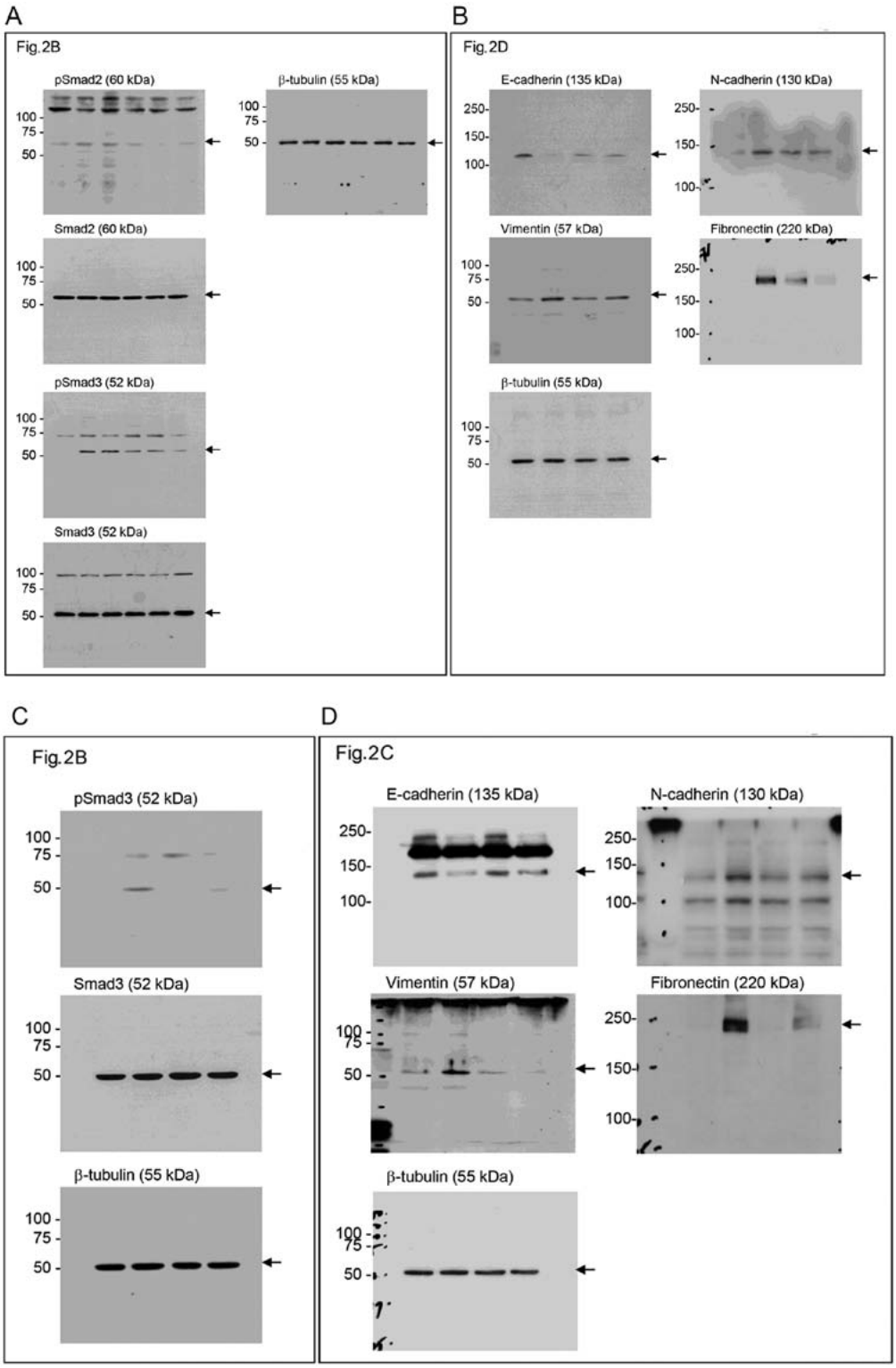

Figure S2. Quantitative representation of western blots. (A-K) Quantitative representations of (A and B) Fig. 2B, (C-F) Fig. 2D, (G) Fig. 3B and (H-K) Fig. 3C are presented. Data are expressed as the mean ± SEM. *P<0.05, **P<0.01, ***P<0.005. TGFβ, transforming growth factor β; 2F-PAF, 2F-peracetyl-fucose; p, phosphorylated.

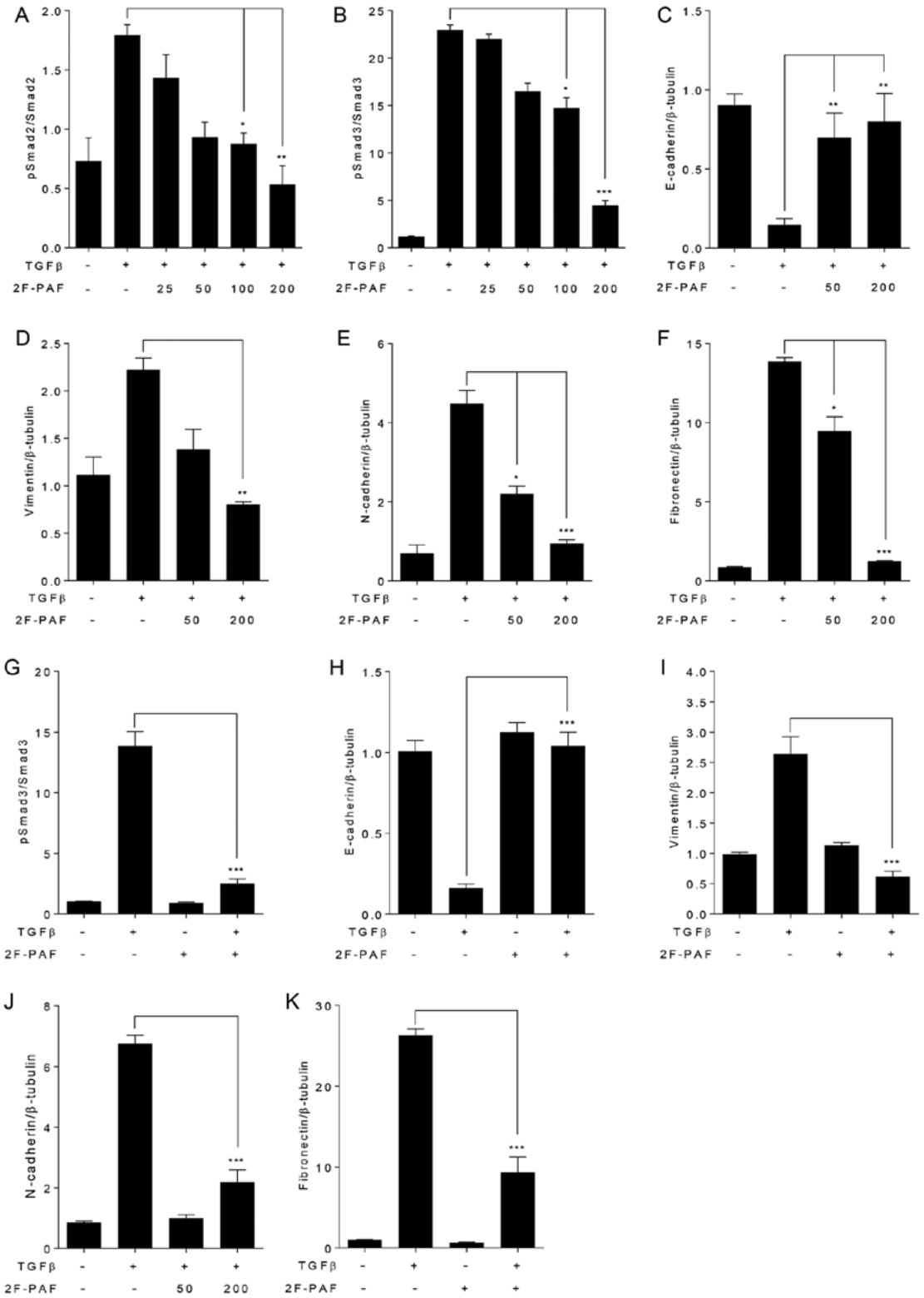

Figure S3. Expression of fucosylation pathway genes in NSCLC. (A) The heatmap of the log_2-transformed expression levels of fucosylation pathway genes in each microarray sample of the GSE19188 dataset. (B) The normalized expression levels of fucosylation pathway genes in patients with NSCLC. Data are expressed as the mean ± SEM and were analyzed using an unpaired t-test. $^{*}P<0.05$, $^{**}P<0.01$, $^{***}P<0.005$. NSCLC, non-small cell lung cancer; FUT, fucosyltransferase; TSTA3, GDP-L-fucose synthase; GMDS, GDP-mannose 4,6-dehydratase; FUK, L-fucose kinase; FPGT, fucose-1-phosphate guanylyltransferase; SLC35C1, GDP-fucose transporter 1; POFUT, protein *O*-fucosyltransferase.

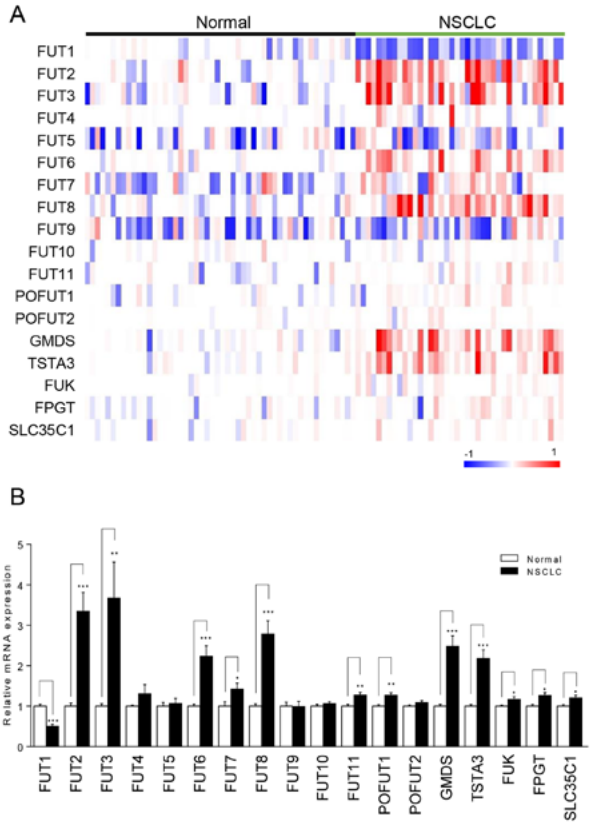

Figure S4. Expression levels of fucosylation pathway genes in each molecular subtype of non-small cell lung cancer. The expression levels of the microarray samples (GSE31210) are presented as boxplots. The upper hinge and lower hinge represent the upper and lower quartiles, respectively. The box is divided by the median, and Tukey-style whiskers are used. (A) FUT1, (B) FUT2, (C) FUT3, (D) FUT4, (E) FUT5, (F) FUT6, (G) FUT7, (H) FUT8, (I) FUT9, (J) FUT10, (K) FUT11, (L) POFUT1, (M) POFUT2, (N) GMDS, (O) TSTA3, (P) FUK, (Q) FPGT, and (R) SCL35C1. FUT, fucosyltransferase; TSTA3, GDP-L-fucose synthase; GMDS, GDP-mannose 4,6-dehydratase; FUK, L-fucose kinase; FPGT, fucose-1-phosphate guanylyltransferase; SLC35C1, GDP-fucose transporter 1; POFUT, protein *O*-fucosyltransferase; N, normal control; TN, triple-negative; EGFR, epidermal growth factor receptor; EML4-ALK, echinoderm microtubule-associated protein-like 4-anaplastic lymphoma kinase fusion. Data are expressed as the means ± SEM. *P<0.05, **P<0.01, ***P<0.005.

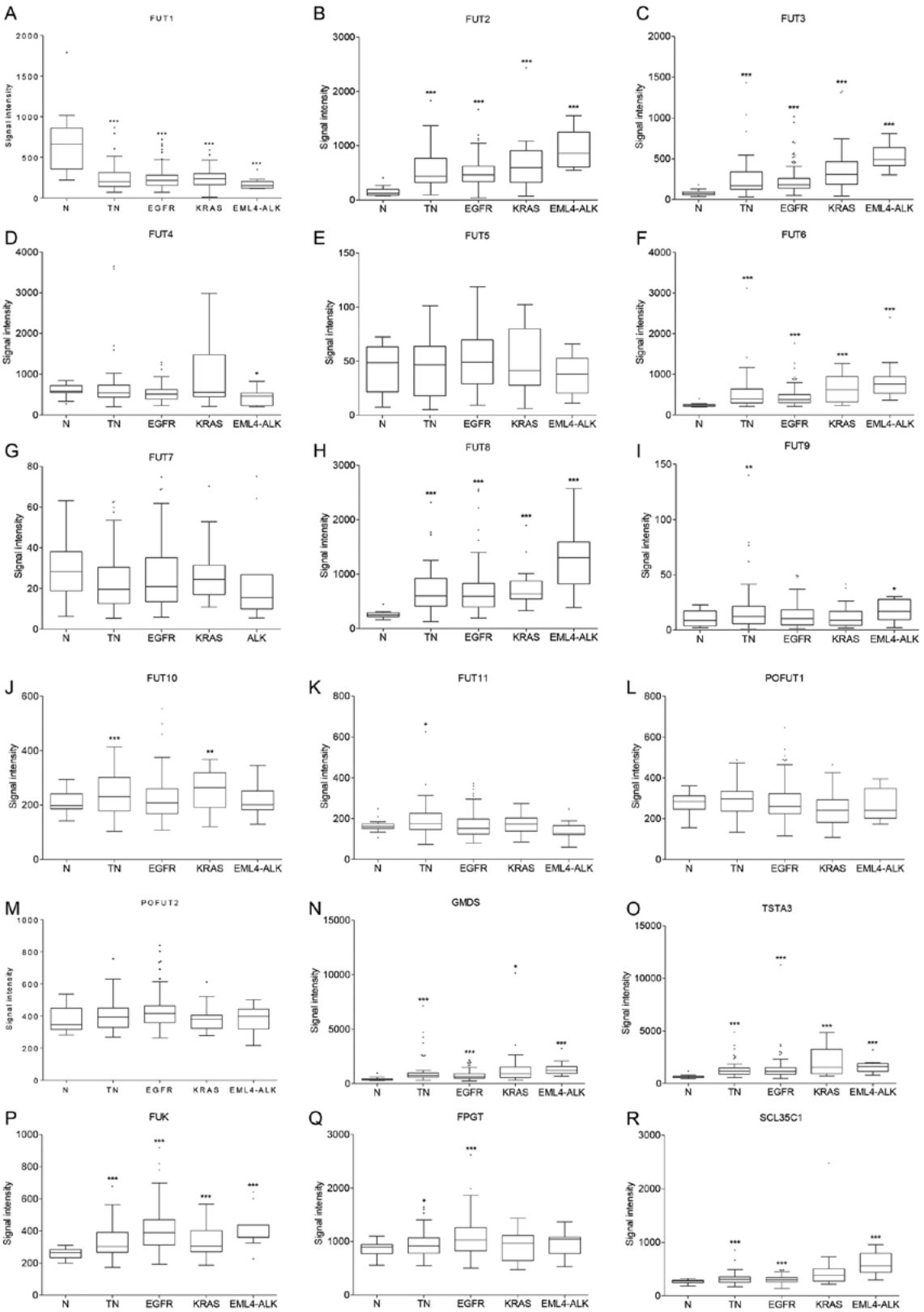

Figure S5. Kaplan-Meier survival curve of patients with NSCLC. Relapse-free survival curves for patients with NSCLC (GSE31210) based on the expression levels [Q1 (n=54), Q2 (n=55), Q3 (n=54) and Q4 (n=54)] of fucosylation pathway genes are presented. (A) FUT1, (B) FUT2, (C) FUT3, (D) FUT4, (E) FUT5, (F) FUT6, (G) FUT7, (H) FUT8, (I) FUT9, (J) FUT10, (K) FUT11, (L) POFUT1, (M) POFUT2, (N) GMDS, (O) TSTA3, (P) FUK, (Q) FPGT, and (R) SCL35C1. NSCLC, non-small cell lung cancer; FUT, fucosyltransferase; TSTA3, GDP-L-fucose synthase; GMDS, GDP-mannose 4,6-dehydratase; FUK, L-fucose kinase; FPGT, fucose-1-phosphate guanylyltransferase; SLC35C1, GDP-fucose transporter 1; POFUT, protein *O*-fucosyltransferase; Q, quartile.

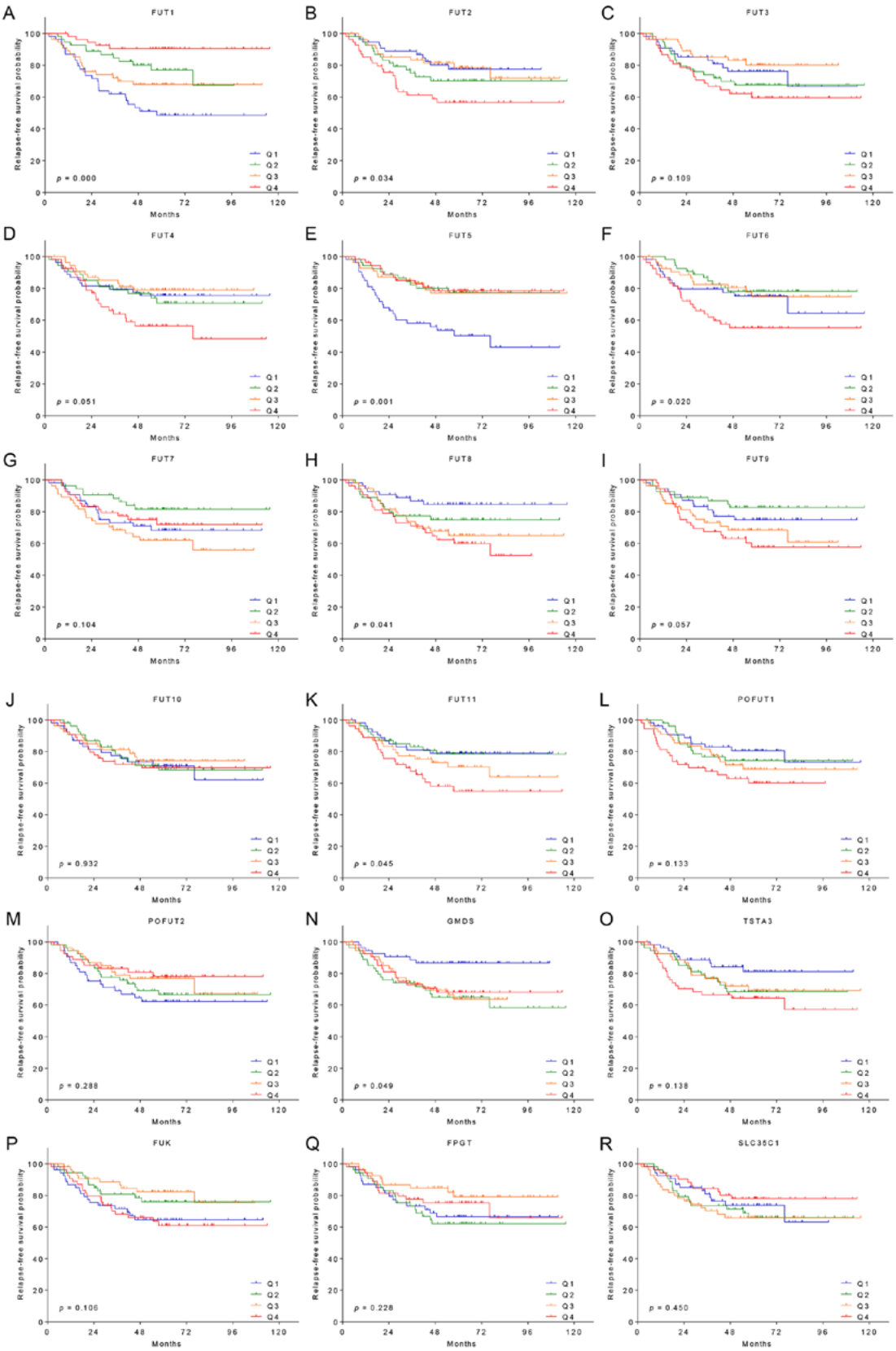

Figure S6: Kaplan-Meier survival curve of patients with NSCLC. Overall survival curves for patients with NSCLC (GSE30219) based on the expression level of fucosylation pathway genes are presented. (A) FUT1, (B) FUT2, (C) FUT3, (D) FUT4, (E) FUT5, (F) FUT6, (G) FUT7, (H) FUT8, (I) FUT9, (J) FUT10, (K) FUT11, (L) POFUT1, (M) POFUT2, (N) GMDS, (O) TSTA3, (P) FUK, (Q) FPGT, and (R) SCL35C1. NSCLC, non-small cell lung cancer; FUT, fucosyltransferase; TSTA3, GDP-L-fucose synthase; GMDS, GDP-mannose 4,6-dehydratase; FUK, L-fucose kinase; FPGT, fucose-1-phosphate guanylyltransferase; SLC35C1, GDP-fucose transporter 1; POFUT, protein *O*-fucosyltransferase.

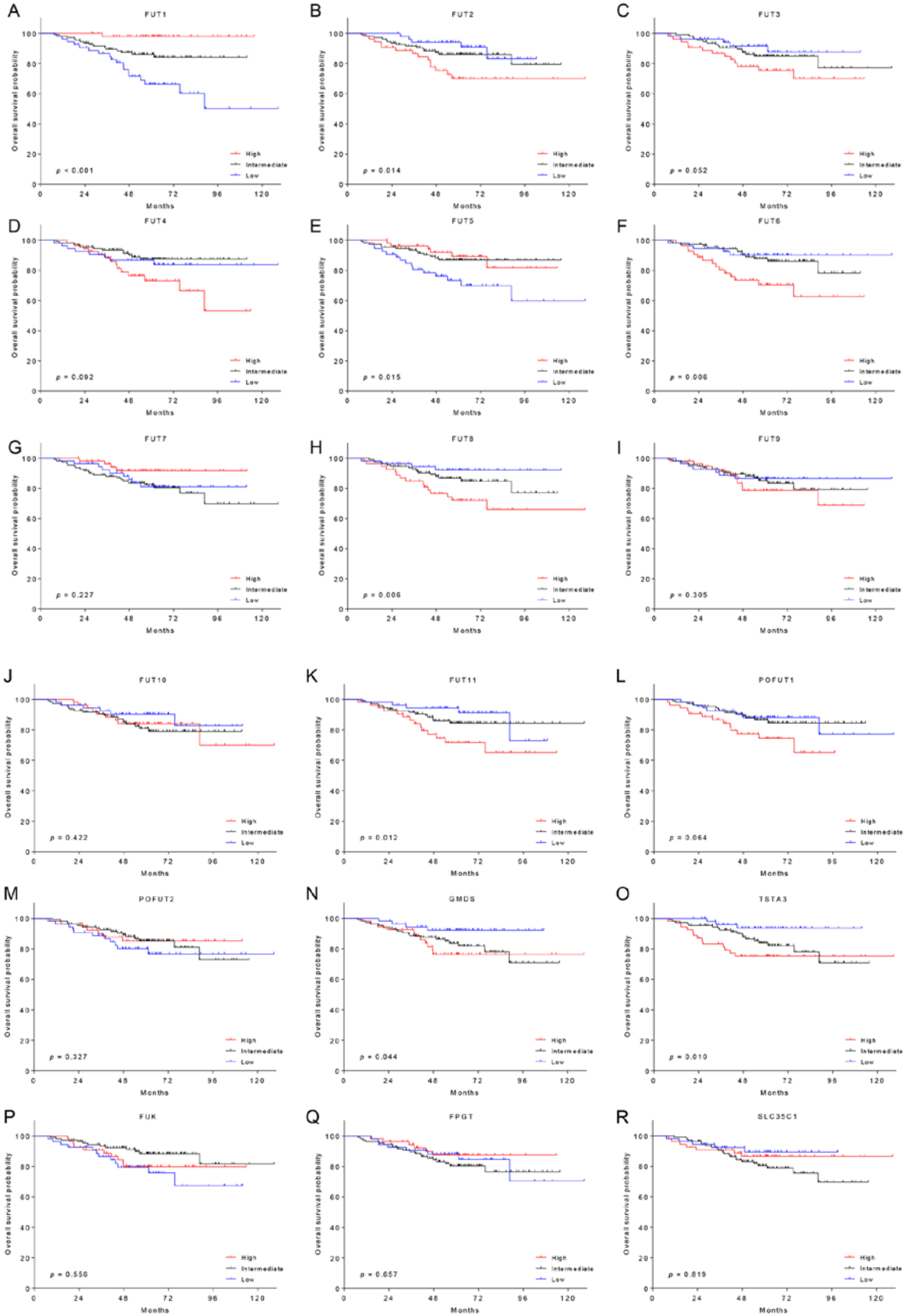

Figure S7. Correlation heatmap of fucosylation pathway genes and transforming growth factor β receptor complex pathway genes in patients with lung adenocarcinoma in the GSE31210 dataset.

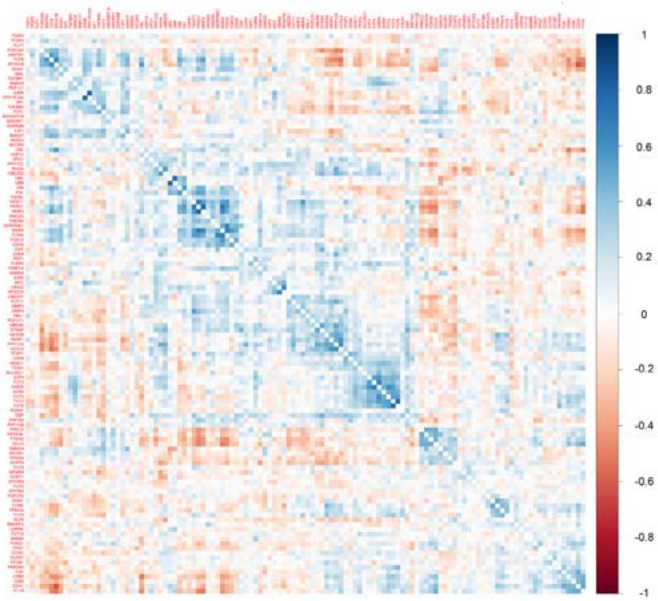

Figure S8. A simple regression model of pairs of FUT and TGFβ receptor complex pathway genes in patients with lung adenocarcinoma in GSE31210. (A) E2F4-FUT4, (B) E2F4-GMDS, (C) CDH1-FUK, (D) SOX9-FUT2, (E) CBL-FUT2, (F) WWTR1-FUK, (G) ZFHX1B-TSTA3 and (H) ZFHX1B-FUT3. FUT, fucosyltransferase; CBL, cbl proto-oncogene; CDH1, cadherin1; E2F4, E2F transcription factor 4; SOX9, SRY-box transcription factor 9; WWTR1, WW domain containing transcription regulator 1; ZFHX1B, zinc finger E-box binding homeobox 2; ZFYVE9, zinc finger FYVE-type Containing 9.

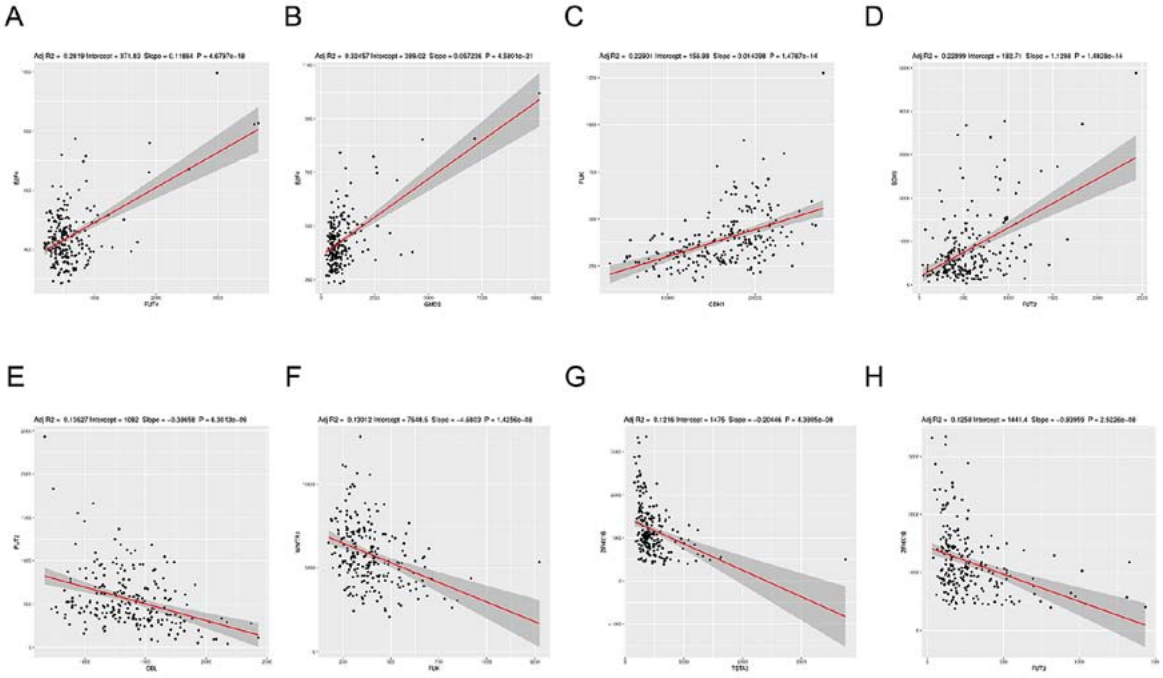

Figure S9. 2F-PAF does not affect NCI-H3122 and Calu-1 cell viability. (A) NCI-H3122 and (B) Calu-1 cells were treated with 2F-PAF at the indicated concentrations for 72 h prior to MTT assay. Cell viability was expressed as the relative absorbance value compared with that of the untreated cells. The data are expressed as the mean ± SEM (n=3). 2F-PAF, 2F-peracetyl-fucose.

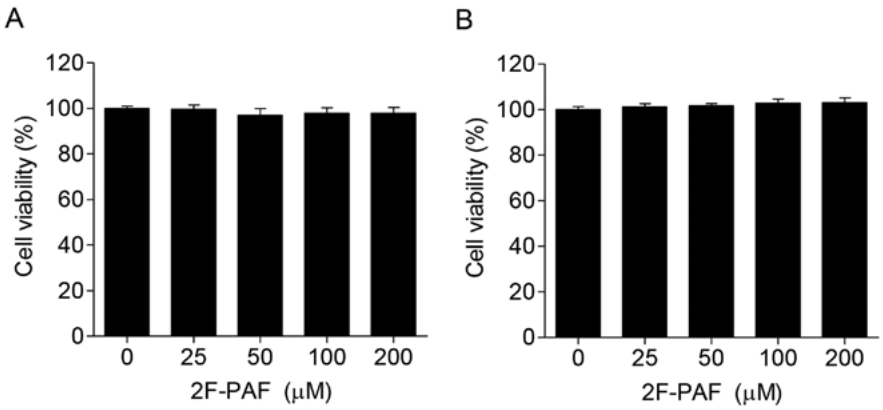

Figure S10. Quantitative representation of the wound-healing cell migration assay. (A-C) Three independent quantitation graphs of Fig. 2E. (D-F) Three independent quantitation graphs of Fig. 3D. The data are expressed as the mean ± SEM (n=3). *P<0.05, **P<0.01, ***P<0.005.

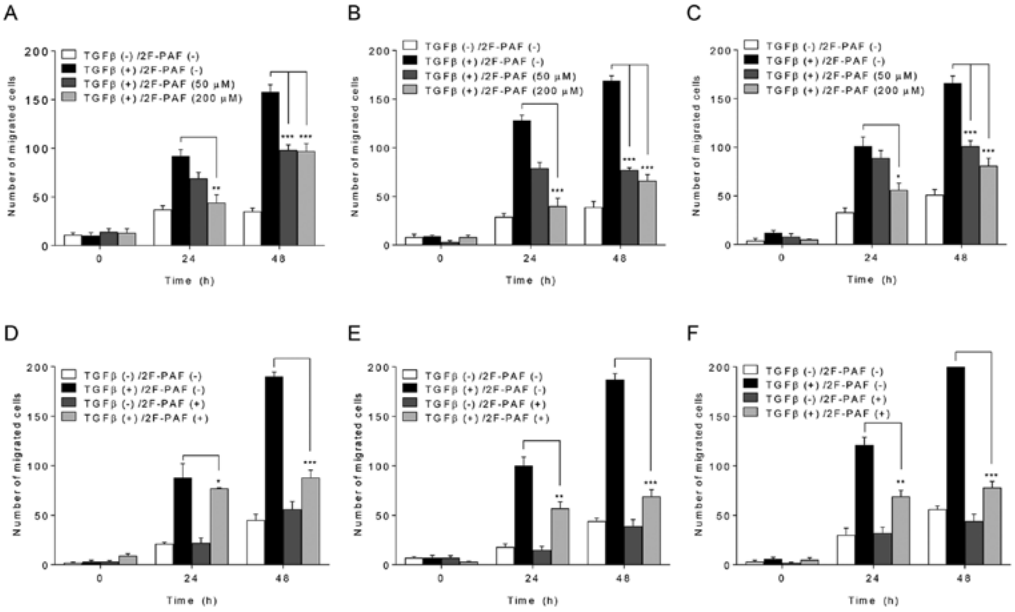

Figure S11. Quantitative representation of the Transwell migration assay. (A-C) Three independent quantitation graphs of Fig. 2F. The data are expressed as the mean ± SEM (n=3). ***P<0.005.